



**HAL**  
open science

## Selective uptake of alkaline earth metals by cyanobacteria forming intracellular carbonates

Nithavong Cam, Karim Benzerara, Thomas Georgelin, Maguy Jaber, Jean-Francois Lambert, Melanie Poinso, Ferial Skouri-Panet, Laure Cordier

► **To cite this version:**

Nithavong Cam, Karim Benzerara, Thomas Georgelin, Maguy Jaber, Jean-Francois Lambert, et al.. Selective uptake of alkaline earth metals by cyanobacteria forming intracellular carbonates. Environmental Science and Technology, 2016, 50 (21), pp.11654-11662. 10.1021/acs.est.6b02872 . hal-01383264

**HAL Id: hal-01383264**

**<https://hal.sorbonne-universite.fr/hal-01383264>**

Submitted on 18 Oct 2016

**HAL** is a multi-disciplinary open access archive for the deposit and dissemination of scientific research documents, whether they are published or not. The documents may come from teaching and research institutions in France or abroad, or from public or private research centers.

L'archive ouverte pluridisciplinaire **HAL**, est destinée au dépôt et à la diffusion de documents scientifiques de niveau recherche, publiés ou non, émanant des établissements d'enseignement et de recherche français ou étrangers, des laboratoires publics ou privés.

1            Selective uptake of alkaline earth metals by  
2            cyanobacteria forming intracellular carbonates

3  
4            Nithavong Cam,<sup>†,‡</sup> Karim Benzerara<sup>\*,†</sup>, Thomas Georgelin,<sup>‡</sup> Maguy Jaber,<sup>§</sup> Jean-François  
5            Lambert,<sup>‡</sup> Mélanie Poinsoy,<sup>†,‡</sup> Fériel Skouri-Panet<sup>†</sup>, Laure Cordier<sup>#</sup>

6            <sup>†</sup> Institut de Minéralogie, de Physique des Matériaux, et de Cosmochimie (IMPMC), Sorbonne  
7            Universités, UPMC Univ Paris 06, UMR CNRS 7590, Muséum National d'Histoire Naturelle, IRD  
8            UMR 206, 4 Place Jussieu, 75005 Paris, France

9            <sup>‡</sup> Laboratoire de Réactivité de Surface (LRS), Sorbonne Universités, UMR CNRS 7197, UPMC  
10            Univ Paris 06, 4 Place Jussieu, 75005 Paris, France

11            <sup>§</sup> Laboratoire d'Archéologie Moléculaire et Structurale (LAMS), Sorbonne Universités, UMR  
12            CNRS 8220, UPMC Univ Paris 06, 4 Place Jussieu, 75005 Paris, France

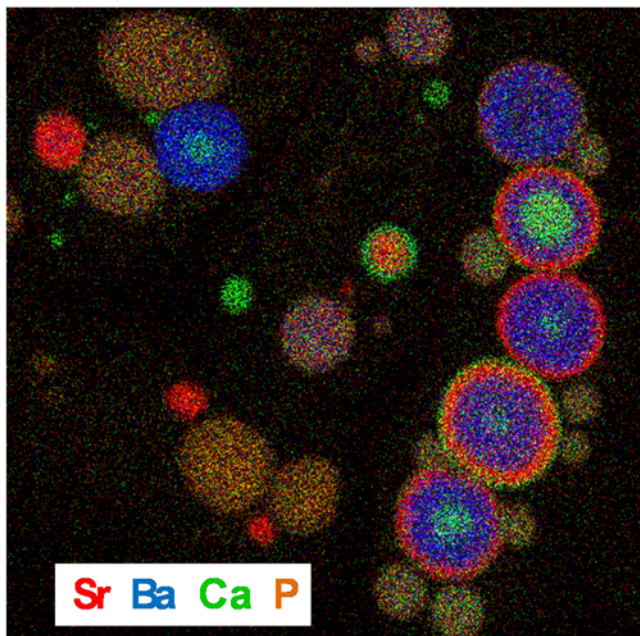
13            <sup>#</sup> Institut de Physique du Globe de Paris (IPGP), Sorbonne Paris Cité – Université Paris Diderot,  
14            UMR CNRS 7154, 1 rue Jussieu, 75238 Paris cedex 05, France

15  
16            \*Corresponding author: [karim.benzerara@upmc.fr](mailto:karim.benzerara@upmc.fr); Phone: +33144277542

18

19

20 TOC/ABSTRACT ART



21

22

23 ABSTRACT

24 The uptakes of Ca, Sr and Ba by two cyanobacterial strains, *Cyanothece sp.* PCC7425 and  
25 *Gloeomargarita lithophora*, both forming intracellular carbonates, were investigated in  
26 laboratory cultures. In the culture medium BG-11 amended with 250  $\mu\text{M}$  of Ca and 50 or 250  
27  $\mu\text{M}$  of Sr and Ba, *G. lithophora* accumulated first Ba, then Sr and finally Ca. Strontium and  
28 barium were completely accumulated by *G. lithophora* cells at rates between 0.02 and 0.10  
29  $\text{fmol}\cdot\text{h}^{-1}\cdot\text{cell}^{-1}$  and down to extracellular concentrations below the detection limits of ICP-AES.  
30 Accumulation of Sr and Ba did not affect the growth rate of the strain. This sequential  
31 accumulation occurred mostly intracellularly within polyphosphate and carbonate granules  
32 and resulted in the formation of core-shell structures in carbonates. In contrast, *Cyanothece*  
33 *sp.* PCC7425 showed neither a preferential accumulation of heavier alkaline earth metals nor

34 core-shell structures in the carbonates. This indicated that fractionation between alkaline  
35 earth metals was not inherent to intracellularly calcifying cyanobacteria but was likely a  
36 genetically-based trait of *G. lithophora*. Overall, the capability of *G. lithophora* to sequester  
37 preferentially Sr and Ba at high rates may be of considerable interest for designing new  
38 remediation strategies and better understanding the geochemical cycles of these elements.

39

40

## 41 INTRODUCTION

42 Alkaline earth metals are lithophile elements with diverse abundances in the Earth. Strontium  
43 (Sr) has an average concentration of 316 ppm in the upper continental crust and 8.1 mg/L in  
44 oceans.<sup>1,2</sup> It is cycled by living organisms with diverse impacts on their biology. Sr is  
45 incorporated by plants, usually at the same rate as calcium (Ca), and can, at least in some  
46 cases, replace Ca to promote plant growth.<sup>3,4</sup> At a low concentration, Sr stimulates bone  
47 formation and can be useful against osteoporosis.<sup>5,6</sup> But at greater doses, Sr inhibits bone  
48 growth and can cause osteomalacia.<sup>7</sup> Strontium 89 and 90 are major polluting nuclear fission  
49 products in environments contaminated by nuclear weapons tests and nuclear reactors  
50 accidents such as the ones of Fukushima or Chernobyl.<sup>8,9</sup> Several (bio-)remediation strategies  
51 have therefore been developed to mitigate Sr dispersion and diverse (micro)organisms with  
52 unique bioremediation capabilities have been screened.<sup>10-12</sup> Barium (Ba), has also received  
53 particular attention regarding its toxicity, in particular in the context of sludge deposits formed  
54 during oil production, which can contain high Ba concentrations.<sup>13,14</sup> For example, Ba in its  
55 ionic form blocks Na-K pumps in cell membranes causing muscular paralysis in animals.<sup>15,16</sup>  
56 Strontium and Ba have also been used as tracers for various (bio)geochemical processes. For  
57 example, Sr/Ca and Ba/Ca ratios have been suggested as good indicators for trophic level in

58 foodwebs in terrestrial environments.<sup>17</sup> Ba/Ca in otoliths has been used to infer where fish  
59 have lived.<sup>18</sup> The Ba/Ca ratio in foraminifers and other biomineralized carbonates has been  
60 used to trace past river discharge in the ocean.<sup>19</sup> Finally, in oceans, pelagic barite (BaSO<sub>4</sub>),  
61 formed in the water column, records changes in ocean productivity.<sup>20-22</sup> Yet, the mechanisms  
62 of precipitation of pelagic barite and the microorganisms mediating this precipitation process  
63 are not known.<sup>23</sup> Recent studies exploring the possibility to use Ba stable isotopes for  
64 deciphering the global Ba cycle call for further efforts to identify the biological processes  
65 affecting this element.<sup>21,22</sup> Overall, there is a crucial need to better understand the  
66 biogeochemical cycle of Sr and Ba in order to strengthen the use of these proxies on one hand  
67 and design remediation strategies on the other hand.<sup>24</sup>

68 Several organisms able to trap Sr and/or Ba have been discovered, including some bacteria,  
69 micro-algae and plants.<sup>11,25-35</sup> Different mechanisms of sequestration may be involved. First,  
70 Sr<sup>2+</sup> and Ba<sup>2+</sup> may be adsorbed on the cell surface.<sup>25</sup> Some organisms such as the algae  
71 *Scenedesmus spinosus* and *Oedogonium* sp. Nak 1001, the cyanobacteria *Oscillatoria*  
72 *homogenea* and *Stigonema ocellatum* NIES-2131 and the aquatic plant *Egeria densa* We2  
73 show a particularly high affinity for Sr, assigned to both sorption at the surface of the  
74 organisms (biosorption) and sequestration within the cells (bioaccumulation). (Fukuda, 2014;  
75 Dabbagh, 2007; Liu, 2014)<sup>11,26,27</sup> The argument for sorption has been based on more or less  
76 complex modeling of the metal sequestration data;<sup>27</sup> in simple cases, fixed amounts were  
77 fitted with a Langmuir isotherm.<sup>26</sup> However, some of these results should be considered with  
78 caution, since deciphering the amount of earth alkaline element uptake and adsorption by  
79 microorganisms is sometime difficult. For example, Sternberg et al.<sup>36</sup> showed that the  
80 apparent uptake of Ba by diatoms in laboratory cultures was actually due to sorption on Fe-  
81 oxyhydroxides formed in the cultures and not uptake by the cells.

82 In other cases, alkaline earth metals are coprecipitated in minerals formed by organisms or  
83 adsorbed on the surfaces of these minerals. For example, the micro-alga *Chlorella vulgaris* and  
84 the bacteria *Sporosarcina pasteurii* (ATC 11 859) and *Halomonas* sp. induce extracellular  
85 precipitation of strontianite ( $\text{SrCO}_3$ ).<sup>28,30,31</sup> In all these cases, the efficiency of Sr and/or Ba  
86 sequestration depends on the chemical conditions prevailing in the extracellular solution,  
87 including pH or the saturation of the solution with concerned mineral phases. These phases  
88 tend to incorporate Ca in addition to Sr and Ba, depending on their concentrations in the  
89 extracellular solution and the relative solubilities of Ca-, Sr- and Ba-mineral phases.

90 In contrast, some organisms accumulate Sr or Ba mostly intracellularly. The efficiency of the  
91 accumulation may depend less on the chemical conditions in the extracellular solution but  
92 more on the physiological status of the cells.<sup>37</sup> For example, the yeast *Saccharomyces*  
93 *cerevisiae* traps  $\text{Sr}^{2+}$  within its vacuole, with Sr uptake involving similar molecular routes as  
94 those for  $\text{Ca}^{2+}$  transport.<sup>38</sup> Interestingly, it has been shown that some organisms accumulate  
95 different alkaline earth metals in proportions that differ from those in the external solution.  
96 For example, Sr/Ca and Ba/Ca ratios measured in the algae *Bryopsis maxima* were significantly  
97 higher than in the extracellular solution.<sup>34</sup> Last but not least, the desmid *Closterium*  
98 *moniliferum* forms barite ( $\text{BaSO}_4$ ) and celestite ( $\text{SrSO}_4$ ) within its vacuole by concentrating  
99 preferentially Sr and Ba over Ca.<sup>35</sup> This was explained by the lower solubilities of barite and  
100 celestite compared to calcium sulfate dihydrate. Radiolarians,<sup>39</sup> green algae of the genus  
101 *Chara*,<sup>40</sup> the ciliate genus *Loxodes*<sup>41</sup> and xenophyophores (a group of foraminifers) are  
102 additional examples of organisms accumulating Sr and/or Ba as sulfates.<sup>42</sup> This selectivity is of  
103 high interest since it may offer strategies to remediate more efficiently Sr and/or Ba from  
104 Ca-rich effluents. Moreover, some of these microorganisms have been suggested to drive the  
105 formation of pelagic barite in oceans, although their abundance may be too low.<sup>23</sup>

106 Interestingly, most of the organisms studied so far showing this selectivity upon alkaline earth  
107 metal uptake are eukaryotes. Therefore, the recently discovered cyanobacterium  
108 *Gloeomargarita lithophora* may provide an original model in this context.<sup>43</sup> Indeed,  
109 *G. lithophora* cells form intracellular Ca-, Sr- and Ba-carbonate granules in solutions containing  
110 a relatively high Ca concentration of 50  $\mu\text{M}$  and low Ba and Sr concentrations of 0.001 and  
111 0.013  $\mu\text{M}$ , respectively. This preferential uptake of Sr and Ba over Ca by *G. lithophora* was  
112 suggested based on electron microscopy observations of a highly diverse microbial  
113 assemblage.<sup>43</sup> *G. lithophora* can accumulate a large amount of alkaline earth metal up to  
114 several fmoles per cell.<sup>44</sup> However, no detailed study has been performed yet on the uptake  
115 kinetics of Sr and Ba by isolated *G. lithophora* cells in a controlled culture medium.

116 The origin of this differential fractionation of alkaline earth metals remains enigmatic for  
117 *G. lithophora*. *In vitro* abiotic syntheses of carbonates similar to the granules observed in  
118 cyanobacteria showed no differential fractionation of Ca, Sr and Ba between the solution and  
119 the mineral phase.<sup>45</sup> This suggested that biological processes rather than physicochemical  
120 parameters, such as solubility differences between alkaline earth carbonates and/or different  
121 precipitation kinetics are responsible for this selectivity between alkaline earth metals in *G*  
122 *lithophora* cells. However, it is not known whether this selectivity is intrinsically related to the  
123 capability of *G. lithophora* to form intracellular carbonates. Interestingly, some other  
124 cyanobacterial species, phylogenetically distant from *G. lithophora* but forming intracellular  
125 carbonates,<sup>46</sup> were recently discovered but their capability to selectively sequester Sr and Ba  
126 over Ca has not been tested yet. If they showed such a capability, they may play a yet  
127 overlooked role in Ba and Sr geochemical cycles since they have been found in many locations  
128 worldwide and diverse continental environments.<sup>47</sup>

129 Here, we followed the time-evolution of the uptake of Ca, Sr and Ba by cells of *G. lithophora*  
130 and *Cyanothece* sp. PCC 7425 cultured in BG-11 amended with Sr and Ba. Both cyanobacterial  
131 strains form intracellular carbonate granules. We quantified and compared the uptakes of Ba,  
132 Sr and Ca by the two cyanobacterial strains and assessed their cellular distributions.

133

## 134 EXPERIMENTAL

135

### 136 **Cyanobacterial strains and culture conditions**

137 Two cyanobacterial strains were tested for Sr and Ba uptake: 1) *Gloeomargarita lithophora* C7  
138 enriched and described by Couradeau et al.<sup>43</sup> and Benzerara et al.<sup>46</sup>; 2) the axenic strain  
139 *Cyanothece* sp. PCC 7425 was obtained from the Pasteur Collection of Cyanobacteria.<sup>48</sup>

140 Both strains were cultured in BG-11 medium at 30 °C under continuous light (5-10  $\mu\text{mol.m}^{-2}.\text{s}^{-1}$ ).<sup>48</sup> BG-11 medium contained 17.65 mM of  $\text{NaNO}_3$ , 0.18 mM of  $\text{K}_2\text{HPO}_4$ , 0.3 mM of  $\text{MgSO}_4$ ,  
141 0.25 mM of  $\text{CaCl}_2$ , 0.03 mM of citric acid, 0.03 mM of ferric ammonium citrate, 0.003 mM  
142 EDTA, 0.38 mM of  $\text{Na}_2\text{CO}_3$ , and trace minerals.<sup>48</sup> Strontium and barium were added to BG-11  
143 as chloride salts (Sigma Aldrich) at final concentrations of 50 or 250  $\mu\text{M}$ . Sulfates may affect  
144 the solubility of Sr and Ba. However, this did not seem to play a significant role in their  
145 bioavailability here since: 1) measured dissolved Sr and Ba concentrations at t=0 (i.e., when  
146 cultures were inoculated) were approximately similar to added ones; 2) Sr and Ba were clearly  
147 incorporated by cyanobacteria as shown by microscopy analyses and 3) the changes with time  
148 of dissolved Sr and Ba concentrations were very different between strains suggesting that  
149 concentrations of Sr and Ba were not buffered by the precipitation of earth alkaline sulfates  
150 in the culture medium. Evaporation was compensated by daily addition of sterile milli-Q  
151 water. The optical density (OD) of the suspensions was measured at 730 nm. The precision on  
152



153 OD measurements was 0.005. The relationships between OD and cell density were estimated  
154 as  $9 \times 10^7$  and  $3 \times 10^7$  cell.mL<sup>-1</sup>.OD unit<sup>-1</sup> for *G. lithophora* and *Cyanothece* sp., respectively. The  
155 relation between OD and cell dry mass was  $3.65 \times 10^{-4}$  g.OD unit<sup>-1</sup> for 1 mL of *G. lithophora*  
156 culture.

157 For bulk chemical analyses, 500 µL of culture were centrifuged at 5,000 g for 10 min. The pH  
158 of the supernatant was systematically measured. The precision on pH measurement was 0.01.  
159 Time variations of the pH in non-inoculated sterile controls were up to 0.1 pH units.  
160 Supernatants were then filtered at 0.22 µm and acidified by addition of 2 µL of HNO<sub>3</sub> (70 %)  
161 in order to measure dissolved Ca, Sr and Ba concentrations. For scanning transmission  
162 electron microscopy (STEM) observations, cell pellets were washed three times with milli-Q  
163 water before suspension in 500 µL of milli-Q water and deposition of 3 µL on carbon-coated  
164 200-mesh copper grids.

#### 165 **ICP-AES measurements**

166 Concentrations of dissolved Ca, Sr, Ba were measured using a Thermo Scientific™ iCAP™ 6200  
167 ICP emission spectrometer equipped with a cetac ASX-520 autosampler. Ten milliliters of 2 %  
168 HNO<sub>3</sub> were added to 300 µL of acidified supernatants. Taking into account dilutions of the  
169 samples before ICP-AES measurements, detection limits for Ca, Sr and Ba concentrations were  
170 0.37, 0.05 and 0.07 µM, respectively.

171 Uptake rates normalized by the number of cells were determined for each time step as

172 followed: 
$$\frac{[X^{2+}]_{t-1} - [X^{2+}]_t}{\text{average cell density between } t_{-1} \text{ and } t} / t - t_{-1}$$

173 Where X denotes one chemical element, t and t-1 are two consecutive sampling times.

174

175 **Scanning transmission electron microscopy (STEM) and energy dispersive x-ray**  
176 **spectrometry (EDXS) analyses**

177 STEM analyses were performed in the high angle annular dark field (HAADF) mode using a  
178 JEOL 2100F operating at 200 kV and equipped with a field emission gun and a JEOL EDXS  
179 detector. Semi-quantitative analyses of EDXS spectra were processed using the JEOL Analysis  
180 Station software following Li et al. procedure.<sup>44</sup> This was based on the use of K-factors. From  
181 this, the atomic percentage of selected element was assessed (here Ca, Mg, Sr and Ba in the  
182 carbonates; Ca, Mg, Sr, Ba, K and P in polyphosphates).

183

## 184 RESULTS AND DISCUSSION

### 185 **Kinetics of Ca, Sr and Ba uptakes by *G. lithophora* and *Cyanothece sp.***

186 *G. lithophora* cells grew with comparable generation times ( $92 \pm 8$  h vs  $108 \pm 2$  h) and up to  
187 similar OD values ( $\sim 0.6$ ) and extracellular pH ( $\sim 9.3$ ) in BG-11 amended with  $50 \mu\text{M}$  Sr and Ba  
188 as in BG-11 without Sr and Ba (Figure S1 ; Table S1).

189 Extracellular concentrations of dissolved Ca, Sr and Ba measured immediately after their  
190 addition to BG-11 were  $236 \pm 8.8$ ,  $45 \pm 0.8$  and  $42 \pm 0.4 \mu\text{M}$ , respectively (Figure 1). The slight  
191 differences with expected concentrations ( $250 \mu\text{M}$ ,  $50 \mu\text{M}$  and  $50 \mu\text{M}$ , respectively) may be  
192 due to dilution errors and/or some sulfate precipitation. The uptake of alkaline earth metals  
193 by *G. lithophora* cells occurred in three consecutive stages. During the first stage, within 175 h,  
194 the concentration of dissolved Ba decreased down to the detection limit ( $0.07 \mu\text{M}$ ). During  
195 this stage, the concentration of Ca decreased by about 10 % only, while the Sr concentration  
196 remained constant. During the second stage, the dissolved Ba concentration remained below  
197 the detection limit, while the Sr concentration decreased down to the detection limit  
198 ( $0.05 \mu\text{M}$ ) in 50 h. During this stage, the concentration of dissolved Ca remained constant.  
199 Finally, in a last stage, the Sr and Ba concentrations remained below detection limits, while

200 the concentration of dissolved Ca decreased down to 43  $\mu\text{M}$  (this value was reached after  
201 384 h of total incubation time). The durations of the different stages varied by 8-31 % between  
202 replicates but they always followed the same order (Figure S2).

203 The uptake rates of alkaline earth metals ranged between 0.02 and 0.10  $\text{fmol}\cdot\text{h}^{-1}\cdot\text{cell}^{-1}$   
204 (Figure S3). Taking replicates into account, average uptake rates were estimated to  
205  $0.058 \pm 0.015 \text{ fmol}\cdot\text{h}^{-1}\cdot\text{cell}^{-1}$  for Ba,  $0.049 \pm 0.021 \text{ fmol}\cdot\text{h}^{-1}\cdot\text{cell}^{-1}$  for Sr and  
206  $0.026 \pm 0.010 \text{ fmol}\cdot\text{h}^{-1}\cdot\text{cell}^{-1}$  of Ca. Uptake rates were therefore in the same order of  
207 magnitude for the different alkaline earth metals, with a slight decrease over the duration of  
208 the culture.

209 In *Cyanothece* sp. PCC 7425 cultures with Sr and Ba at 50  $\mu\text{M}$ , the optical density increased up  
210 to 1 in 350 h, while the pH increased and plateaued at around 9 after 250 hours (Figure S4).  
211 The growth in cultures with Sr and Ba was slightly faster than in cultures without Sr and Ba  
212 (~63 h vs 82 h; Figure S5).

213 The different stages of Ba, Sr and Ca uptake evidenced for *G. lithophora* were not observed  
214 for *Cyanothece* sp. (Figure 2). In contrast, the concentration of dissolved Ca decreased first.  
215 The concentrations of dissolved Sr and Ba only decreased in a later stage, when dissolved Ca  
216 concentration had fallen down to about 50  $\mu\text{M}$ , i.e. similar to initial concentrations of Sr and  
217 Ba.

218 Overall, only *G. lithophora* showed preferential uptakes of Ba over Sr and Sr over Ca. This  
219 selectivity for alkaline earth metals was therefore not related to intracellular carbonate  
220 formation. Based on *in vitro* syntheses, Cam et al.<sup>45</sup> showed that the precipitation of  
221 amorphous carbonates alone could not fractionate significantly Sr, Ba and Ca and suggested  
222 that some other mechanisms must be operating in *G. lithophora*. The present study supports  
223 this hypothesis and reveals that the molecular machinery allowing selective fractionation of

224 alkaline earth metals exists in *G. lithophora* but not *Cyanothece sp.* Interestingly, this process  
225 of alkaline earth metals sequestration by carbonates in solutions undersaturated with Sr and  
226 Ba carbonates was observed in Lake Lemna in relation with the picoplankton.<sup>49</sup> Whether  
227 microorganisms with capabilities similar to those of *G. lithophora* occur in Lake Lemna will  
228 have to be determined in the future.

229

### 230 **Cellular distribution of Ca, Sr and Ba in *G. lithophora* and *Cyanothece sp.***

231 The evolution of the chemical composition of intracellular carbonates was assessed by STEM-  
232 HAADF. At 75 h, i.e., during Ba uptake, *G. lithophora* cells had divided once on average  
233 (Figure 1). The majority of the carbonate granules in the cells (55 % out of 31 observed  
234 granules) showed a bright outer shell around a dark core (Figure 3). Accordingly, EDXS  
235 analyses indicated that the core was rich in Ca and the brighter outer shell was rich in Ba. The  
236 thickness of the Ba-shell measured  $80 \pm 34$  nm (11 analyzed particles). Considering the relative  
237 thicknesses of the shells, the diameters of the cores and the Ca/Ba ratios measured on the  
238 cores (Figure 3), EDXS measurements were consistent with pure Ca-carbonate cores covered  
239 by Ba-carbonate outer shells. Moreover, in the same cells, some carbonate granules (25 %  
240 over 31 counted granules) contained only Ba with no Ca-rich cores, while other granules (20 %  
241 contained only Ca with no outer Ba-carbonate shell. In accordance with bulk chemical analyses  
242 of the solutions, mixed Ca- and Ba-containing carbonate granules were interpreted as  
243 resulting from the growth of Ba-carbonates during the first 75 hours around Ca-carbonate  
244 cores. Ca-carbonate cores formed in the pre-culture grown in Ba- and Sr-depleted BG-11. In  
245 the meantime, some new Ba-carbonate granules nucleated within the cells and some pre-  
246 existing Ca-carbonate granules did not grow further. Two concurrent nucleation pathways  
247 occur for barium carbonates: one forming particles *de novo* by homogeneous (in solution) or

248 heterogeneous (on organic template) nucleation and the other one by heterogeneous  
249 nucleation on the surface of preexisting calcium carbonates. The heterogeneous nucleation is  
250 followed by a two-step growth: very rapid 2-D growth on the underlying particle resulting in  
251 complete coverage, followed by slower growth perpendicular to the surface.

252 Cells contained a volume of  $0.064 \pm 0.043 \mu\text{m}^3 \cdot \text{cell}^{-1}$  of both Ca- and Ba-carbonates on  
253 average. After 75 h of cell growth, there were  $4.57 \times 10^6 \text{ cell} \cdot \text{mL}^{-1}$  in the cultures, accounting  
254 for a total uptake of  $12.75 \times 10^{-9} \text{ mol} \cdot \text{mL}^{-1}$  of Ba, i.e.,  $2.8 \text{ fmol} \cdot \text{cell}^{-1}$  of Ba. If all this Ba was  
255 trapped as carbonates only, this would represent a total volume of  $0.151 \mu\text{m}^3$  per cell based  
256 on a density of  $4.3 \text{ g} \cdot \text{cm}^{-3}$  for amorphous Ba-carbonate.<sup>50</sup> This is significantly more than the  
257 volume of carbonates observed by STEM, suggesting that only a fraction of Ba ( $\sim 1/3$ ) was  
258 contained in carbonate granules.

259 *G. lithophora* cells also contained phosphorus-rich granules (Figure 3), which were identified  
260 as polyphosphates (PolyP) by Li et al.<sup>44</sup> The preferential uptake of Ba over Sr and Ca was not  
261 restricted to carbonate granules only since in addition to Mg, Ca and K, PolyP granules  
262 contained Ba in cells sampled during the Ba uptake stage (Figure 3; Figure S6). Ba content  
263 ranged between 30 and 70 % (expressed as an atomic proportion over Mg+Ca+Sr+Ba) in PolyP.  
264 EDXS maps showed that Ba concentration was high in carbonate and PolyP granules (Figure 3)  
265 but below detection limits in the rest of the cells (Figure 3). Therefore, most of Ba was  
266 accumulated in PolyP and carbonate granules with possibly some minor amount complexed  
267 by proteins.

268 At 244 h, i.e., during the Sr uptake stage (Figure S2), Sr-carbonates were detected within the  
269 cells (Figure 3). Some particles showed a Ca-rich core and two outer superimposed shells, a  
270 Ba-rich intermediate shell and a Sr-rich external shell. Some carbonate granules containing  
271 mostly Sr, with minor amounts of Ca and Ba (Figure 3), were also observed. Polyphosphates

272 granules were homogeneous in composition and contained mostly Mg, K, Sr and Ba,  
273 sometimes with small, almost undetectable amounts of Ca. Their compositions were variable  
274 but most of them showed an increased proportion of Sr (15% on average; Figure S6).

275 Finally, at 310 h, during the Ca uptake stage, granules showed a Ca-rich core and three  
276 successive shells rich in Ba, Sr and Ca, respectively, from the center to the periphery (Figure 3).

277 Other types of granules were observed but always with the same order for the shells, e.g.,  
278 Ca-shells over Sr-cores; Ca-cores only; Sr-shells over Ba-shells. Despite some variability in  
279 chemical composition from cell to cell, polyphosphate granules contained higher  
280 concentrations of Ca than during the Sr uptake stage (27% vs. 6% during the Sr uptake stage;  
281 Figure S6).

282 Overall, we observed in *G. lithophora* cells 1) newly nucleated carbonate granules containing  
283 only one alkaline earth metal, named “simple”, and 2) “composite” carbonate granules with  
284 outer shells containing Ba, Sr or Ca. “Simple” granules had a mean diameter of  $215 \pm 91$  nm  
285 with a normal distribution (Figure S7), very similar to that observed for Ca-carbonate granules  
286 ( $217 \pm 64$  nm) in *G. lithophora* cultured in BG-11 with no Sr and Ba.<sup>44</sup> In contrast, “composite”  
287 granules showed larger diameters, i.e.  $415 \pm 115$  nm, and measured up to 650 nm in diameter  
288 (Figure S7).

289 For a comparison, *Cyanothece sp.* cells were also observed by STEM-HAADF at 244 h, i.e. at a  
290 stage when they were mostly taking up Ca, and at 310 h, i.e. during the Ca, Ba and Sr uptake  
291 stage (Figure 4; Figure S8). In agreement with bulk chemical measurements, intracellular  
292 carbonates within these cells mostly contained Ca ( $82.2 \pm 6.2$  % atomic proportion of Ca over  
293 Mg+Ca+Sr+Ba) with several percent of Sr and Ba (on average 7.8 and 7.3 % at 310 h, of Sr and  
294 Ba respectively). However, in contrast to *G. lithophora*, *Cyanothece sp.* cells showed  
295 chemically homogeneous carbonate granules with no core-shell structure. Polyphosphates

296 also mostly contained Ca with only a few percent of Sr and Ba at 244h (3% of Sr and Ba) and a  
297 slightly higher content in Ba and Sr at 310 h (11 and 5% respectively; Figure S8).

298

### 299 **Origin of selectivity for alkaline earth metals in *G. lithophora***

300 In this study, both *G. lithophora* and *Cyanothece sp.* strains incorporated alkaline earth metals  
301 massively when cultured in BG-11 amended with Sr and Ba. However, only *Gloeomargarita*  
302 *lithophora* achieved a sequential and preferential uptake of Ba over Sr and Sr over Ca. This  
303 was detected by marked changes in the chemical composition of the extracellular solution as  
304 well as in the chemical composition of the intracellular carbonate and polyphosphate  
305 granules.

306 A preferential uptake of Sr and/or Ba over Ca has been observed previously in the desmid  
307 green algae *Closterium moniliferum*.<sup>35</sup> The algae concentrate Ba and Sr in their vacuoles as Ba-  
308 and Sr-sulfate crystals. Based on the large solubility differences of Ca-, Sr- and Ba-sulfates,  
309 Krejci et al.<sup>35</sup> suggested that the preferential uptake of Sr and Ba over Ca was due to an  
310 elemental fractionation induced by sulfate precipitation within the cells. In contrast, several  
311 observations strongly argue against a fractionation of alkaline earth metals by mineral  
312 precipitation in *G. lithophora* and favor the involvement of another biochemical process:  
313 1) Cam et al.<sup>45</sup> showed that the solution/solid fractionations were very similar for Sr, Ba and  
314 Ca for *in vitro* precipitation of amorphous carbonates; 2) no Sr-, Ba and/or Ca-sulfate phase  
315 precursor to the carbonates, which could induce some distinct fractionation between Sr, Ba  
316 and Ca, was observed within *G. lithophora*; 3) the composition of PolyP followed the same  
317 succession of uptake stages as the carbonates; 4) *Cyanothece sp.* did not fractionate Sr, Ba  
318 and Ca distinctly, although it also formed intracellular carbonates.

319 Unfortunately, no biochemical process explaining such a selectivity between alkaline earth  
320 elements is presently known. All known biomolecules have either a similar affinity for Ca and  
321 Sr and a lower affinity for Ba, or a high affinity for Ca and lower affinities for Sr and Ba.<sup>52-56</sup>  
322 Future work based for example on genetics and comparative genomics between strains  
323 incorporating alkaline earth metals selectively and others not able of this selective uptake may  
324 provide some clues about the biochemical origin of this selectivity.

325

### 326 **Implications for bioremediation and the geochemical cycles of Ba and Sr**

327 The masses of intracellular Ba, Ca and Sr in *G. lithophora* cells were estimated as a function of  
328 time and normalized to the total cell dry mass (Figure S9). For Ba, there was first an increase  
329 when uptake was higher than “dilution” by cell division, then a plateau and finally a decrease  
330 when no Ba was left in the extracellular solution but cell division was continuing. Baryum mass  
331 reached a maximum of 16 % of the total cell dry mass. Similar evolutions were observed for  
332 Sr and Ca with a maximum of 7 % for the mass of Sr over the total cell weight.

333 Cultures were also conducted in BG-11 containing higher initial Sr and Ba concentrations  
334 (245  $\mu\text{M}$ ). The pH and the OD increased similarly to what was observed in cultures with 50  $\mu\text{M}$   
335 of Sr and Ba with a slightly longer generation time (Figure S10). Similarly to what was observed  
336 in the presence of 50  $\mu\text{M}$  of Sr and Ba, three uptake stages were detected (Figure S11). The  
337 concentration of dissolved Ba decreased first, and this step was followed by decreases of the  
338 concentrations of dissolved Sr and finally of dissolved Ca. In 650 h, cells took 245  $\mu\text{M}$  of Ba,  
339 245  $\mu\text{M}$  of Sr and 245  $\mu\text{M}$  of Ca. Under these conditions barium and strontium masses reached  
340 up to a maximum of 22 % and 8 % of total cell dry mass, respectively (Figure 5).

341 Altogether, these results show that *G. lithophora* can strongly accumulate Ba and Sr while  
342 staying viable and showing high selective affinity for these alkaline earth metals over Ca.



343 Moreover, this selective uptake seems to operate even at low Sr/Ca or Ba/Ca ratios in the  
344 extracellular solution since Ba and Sr are taken up preferentially down to their detection limits  
345 (0.07 and 0.05  $\mu\text{M}$ , respectively, corresponding to a molar ratio between 2.0 and  $2.9 \times 10^{-4}$  with  
346 respect to Ca).

347 Several micro-organisms have been studied for their capability to store Sr or Ba with the  
348 ultimate scope of designing bioremediation strategies (Table 1). In the present study, only  
349 minimum uptake capabilities were determined for *G. lithophora* since our cultures exhausted  
350 the amount of Sr and Ba provided, without any evidence that they had reached their ultimate  
351 storage capacity. *G. lithophora* showed unique uptake capabilities per cell. For example, a cell  
352 of the desmid *Closterium moniliferum* had greater Sr uptake capability than a cell of  
353 *G. lithophora* (140 vs. 35  $\text{fmol}\cdot\text{cell}^{-1}$ ) but when normalized to the cell mass, *G. lithophora*  
354 showed a much higher uptake (75  $\text{mg}/\text{g}$  vs 2  $\text{mg}/\text{g}$ ).

355 Fukuda et al. (2014)<sup>14</sup> screened 188 different strains of macro- and micro-organisms from  
356 aquatic environments in search for good candidates to bioremediate radionuclide  
357 contaminations, including isotopes of strontium. Cyanobacteria showed particularly high  
358 uptake capabilities (Fukuda, 2014).<sup>14</sup> They suggested that this may be due to some particular  
359 properties of their cell walls without further proof. Cyanobacteria forming intracellular  
360 carbonates, including but not restricted to *G. lithophora*, meet the different criteria  
361 mentioned by Fukuda et al.<sup>11</sup> as good candidates for bioremediation. Moreover, they have  
362 been isolated from different places around the world and can grow at varied temperatures.<sup>46</sup>  
363 Some are thermophilic, some mesophilic; some live in high altitude lakes, while others live in  
364 soils. Among intracellularly calcifying cyanobacteria, *Gloeomargarita lithophora* is particularly  
365 interesting: it preferentially sequesters Ba and Sr over Ca, which offers a unique solution to  
366 the general problem of remediating these pollutants in aqueous environments with naturally

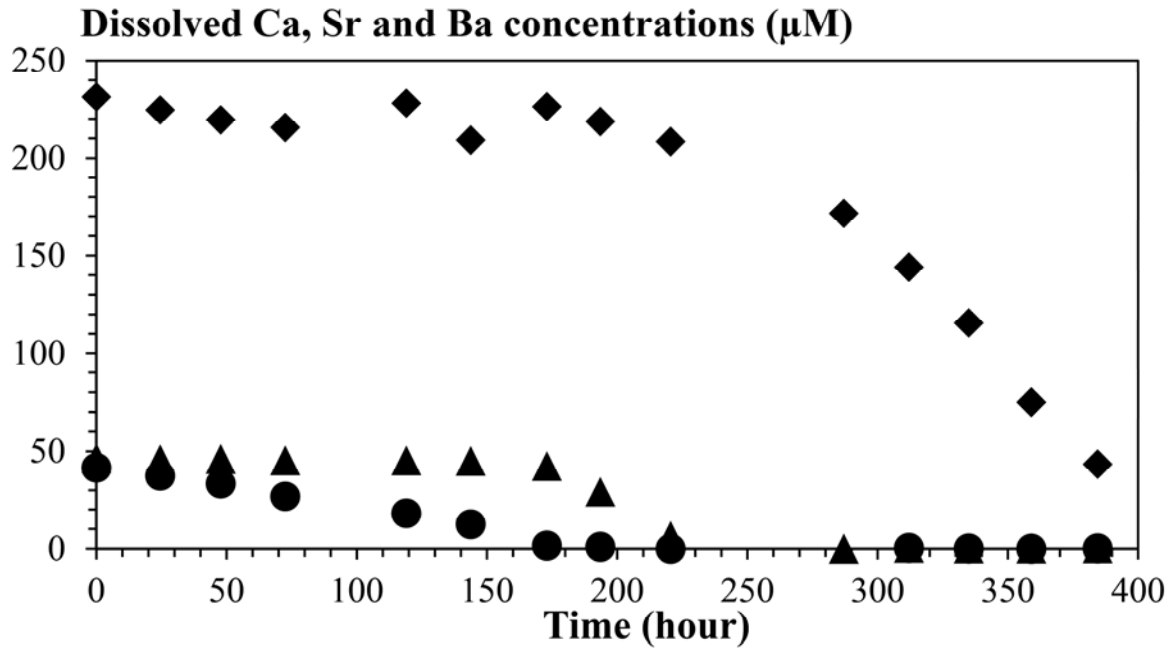
367 high Ca concentrations. However, if cells are used directly in bioremediation strategies,  
368 several parameters will have to be determined in the future to fully assess the potential of  
369 *G. lithophora* such as its maximum uptake capability for Sr and its resistance to radioactivity  
370 from  $^{89}\text{Sr}$  or  $^{90}\text{Sr}$ . Alternatively, it will be important to understand the precise molecular  
371 mechanisms involved in the preferential uptake of Sr and Ba vs Ca which may inspire the  
372 design of new cell-free remediation strategies, complementing those already existing and  
373 using non-biological materials, such as synthetic chelators or ion exchangers.<sup>10</sup>

374 In parallel, the present study has implications for the geochemical cycles of Sr and Ba. First, it  
375 shows that some cyanobacteria concentrate significantly Sr and Ba in connection with the  
376 formation of carbonates and not sulfates as usually considered. With the aim of explaining the  
377 formation of pelagic barite in oceans, Gonzalez-Munoz et al.<sup>57</sup> showed that several  
378 heterotrophic marine bacterial strains could induce the precipitation of barite. However, they  
379 needed to culture them at relatively high Ba concentrations (2 mM). The existence of primary  
380 producers accumulating Ba significantly, such as *G. lithophora* may provide such a rich source  
381 of Ba. Moreover, Peek and Clementz<sup>17</sup> compiled numerous Sr/Ca and Ba/Ca measurements  
382 on biological samples. They suggested that most of the variations of these ratios were  
383 accounted by (abiotic) variations in geochemical sources of alkaline earth metals in terrestrial  
384 environments, while high accumulation of Sr and Ba by microorganisms tended to control  
385 Sr/Ca and Ba/Ca ratios at the base of marine foodwebs. Here, we show that microorganisms  
386 such as *G. lithophora* may play a similar role in continental environments. As a conclusion, the  
387 biochemical process evidenced in *G. lithophora* in the present study might have an important  
388 impact on the geochemical cycles of Sr and Ba if it is widespread. This will need to be assessed  
389 by future studies.

390

391 FIGURES

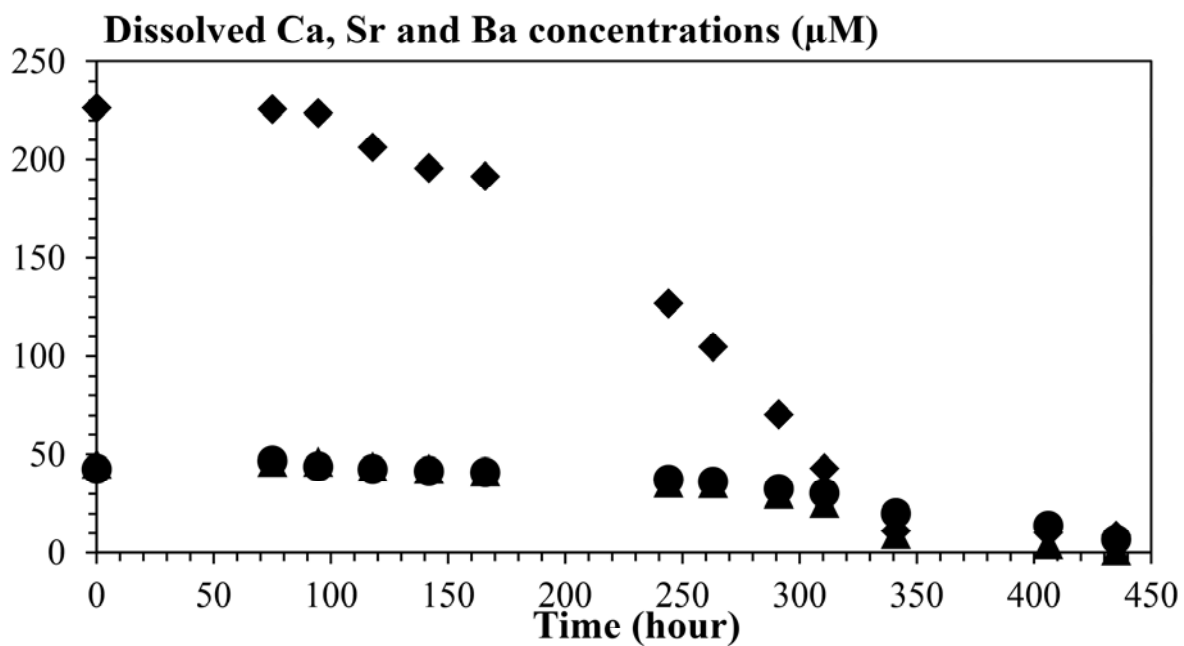
392



393

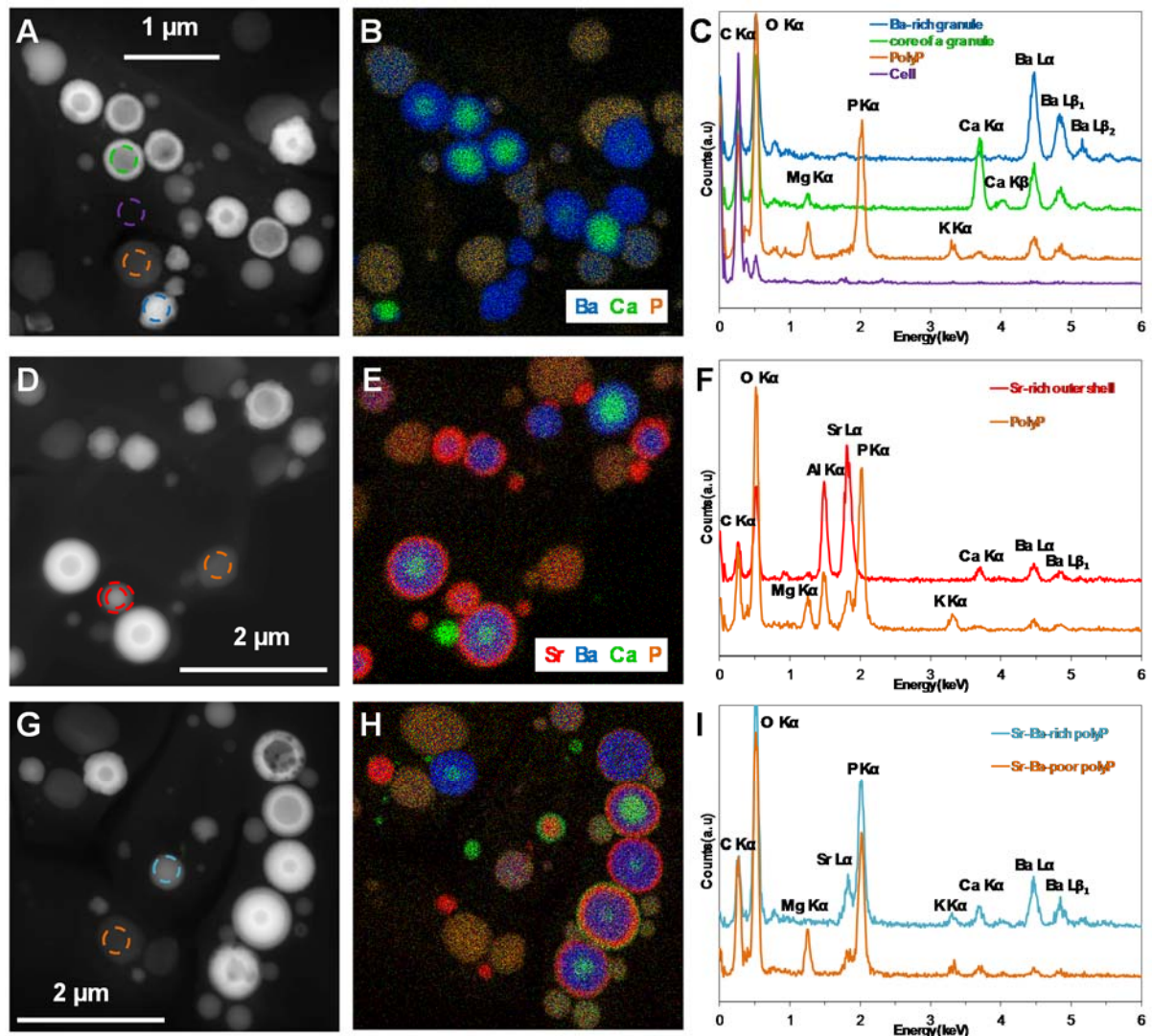
394 **Figure 1.** Time evolution of the concentrations of dissolved Ca (diamonds), Sr (triangles) and  
395 Ba (circles) concentrations in a culture of *Gloeomargarita lithophora* inoculated in  
396 BG-11. Error bars are smaller than symbols.

397



398

399 **Figure 2.** Time evolution of the concentrations of dissolved Ca (diamonds), Sr (triangles) and  
 400 Ba (circles) concentrations in a culture of *Cyanothece* sp. inoculated in BG-11. Analytical  
 401 standard deviations are smaller than the symbol sizes.

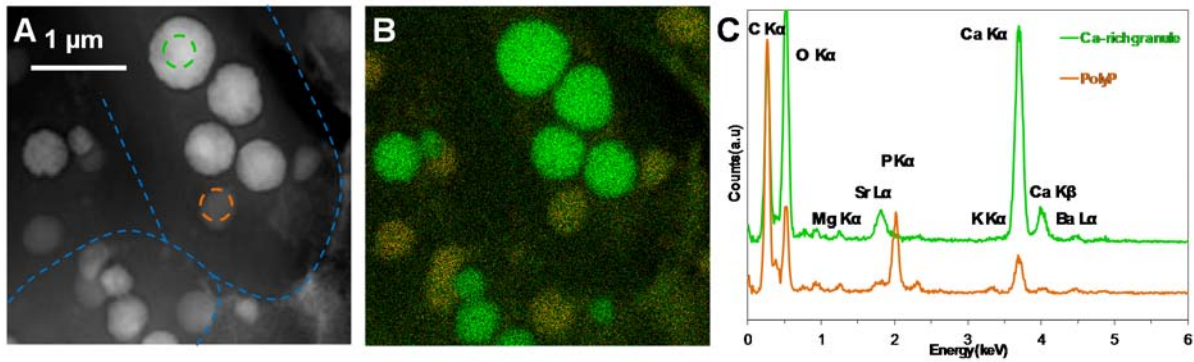


402

403 **Figure 3.** STEM and EDXS analyses of *Gloeomargarita lithophora* cells collected after 75 h  
 404 of culture during the Ba uptake stage (A, B and C), during the Sr uptake stage (D, E and F) and  
 405 during theca uptake stage (G, H and I). (A, D and G) STEM-HAADF Image of cells showing  
 406 layered carbonate granules. Colored circles show the different areas analyzed by EDXS. (B, E  
 407 and H) Corresponding EDXS map of calcium (green), strontium (red), barium (blue) and  
 408 phosphorus (orange). (C) EDXS spectra of the Ba-rich granule; a core of a carbonate granule;  
 409 a PolyP granule and a cellular area comprising no particle shown respectively in A by the blue;  
 410 green; orange and purple circles. (F) EDXS spectra of a Sr-rich outer shell of a granule and a  
 411 PolyP particle shown respectively by the red and the orange circles in D. Al comes from the

412 sample holder.(I) EDX spectra of the PolyP granules shown by the orange and blue circles in  
 413 G.

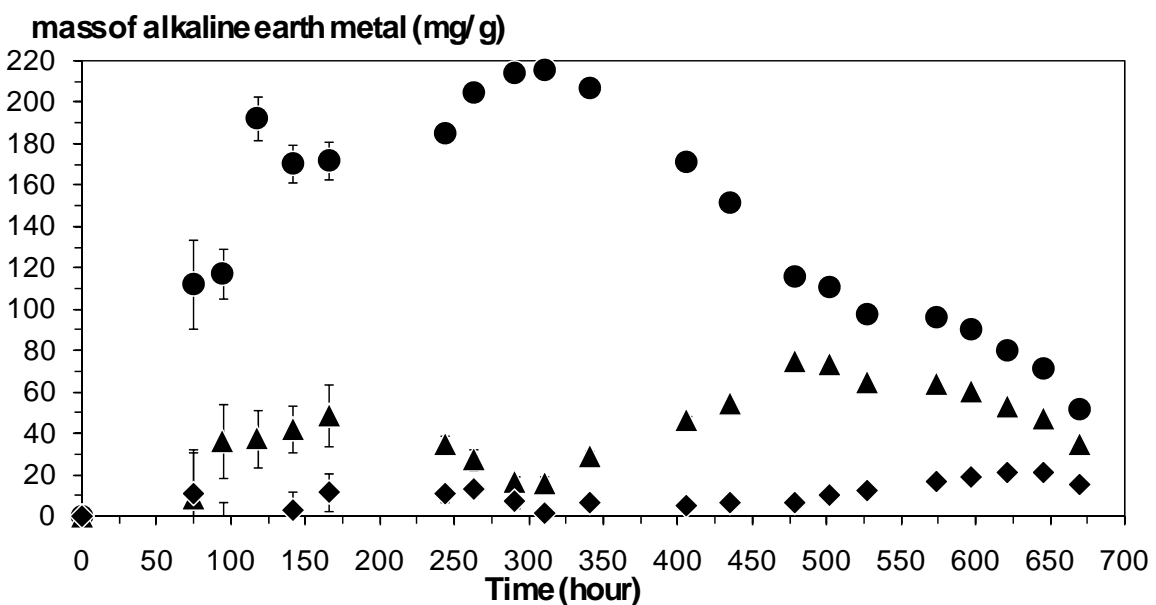
414



415

416 **Figure 4.** STEM analyses of two *Cyanothecce* sp. cells cultured for 310 h in BG-11 medium  
 417 with 50  $\mu\text{M}$  of strontium and 50  $\mu\text{M}$  of barium. (A) STEM image in the HAADF mode. Circles  
 418 indicate the carbonate and PolyP granules on which EDXS spectra shown in C were measured.  
 419 (B) Corresponding EDXS map of calcium (green) and phosphorus (orange). (C) EDX spectra  
 420 of a carbonate granule and of a PolyP granule, respectively shown by the green and the orange  
 421 circles in A.

422



423

424 **Figure 5.** Time evolution of the mass of bioaccumulated Ba (circles), Sr (triangles) and Ca  
 425 (diamonds) per total dry mass of the cells (mg/g) for a culture of *Gloeomargarita lithophora* in  
 426 BG-11 medium with 245  $\mu$ M of strontium and 245  $\mu$ M of barium. When not visible, analytical  
 427 errors bars are smaller than the size of the symbols.

428

429 TABLES

430

Type of organism / material	Name	Maximum uptake rate	Maximum uptake		Maximum remediation		Associated mechanism	References
		(fmol/h/cell)	(mg/g of dry matter)	(fmol/cell)	(%)	( $\mu$ M)		
<b>Strontium</b>								
Non organic material	Layered metal sulfides				99.4	756		13
Aquatic plant	<i>E. densa</i> We2		0.0009		33.9		Adsorption	14
Algae	<i>B. maxima</i>		15.9				Intracellular accumulation	31
Algae	<i>S. spinosus</i>		2.5		76	787	Adsorption	23
Yeast	<i>S. cerevisiae</i>	1.2	20	0.315	85		Intracellular accumulation and adsorption	30,36
Desmid	<i>C. moniliferum</i>	1.7	2*	140			Intracellular sulfate	32,59
Micro-algae	<i>O. sp.</i> Nak 1001		0.0029		36.3		Adsorption	14
Bacterium	<i>H. sp.</i> SR4				80		Extracellular calcite	26
Bacterium	<i>B. pasteurii</i> ATCC 11859				36	40	Extracellular calcite	25
Bacterium	<i>S. pasteurii</i> ATCC 11859				59		Extracellular calcite	27
Cyanobacterium	<i>S. ocellatum</i> NIES 2131		0.0219		41.3		Adsorption	14
Cyanobacterium	<i>N. carneum</i>		0.00225		97.8		Adsorption	21
Cyanobacterium	<i>G. lithophora</i>	0.079	75	35	100	250	Intracellular amorphous carbonates	
<b>Barium</b>								
Algae	<i>B. maxima</i>		3.79				Intracellular accumulation	31
Desmid	<i>C. moniliferum</i>		46*	2112			Intracellular sulfate	60
Cyanobacterium	<i>G. lithophora</i>		220	64	100	250	Intracellular amorphous carbonates	

\*calculated using a cell volume of 125,600  $\mu$ m<sup>3</sup> and Kreger and Boeré (1969).<sup>58</sup>

431

432 Table 1. Remediation capabilities of selected materials and organisms.

433

434 ASSOCIATED CONTENT

435 **Supporting Information**

436 Data on culture replicates, composition of polyphosphate inclusions, size distributions of  
437 carbonate inclusions, data on cultures of *G. lithophora* with 250  $\mu\text{M}$  of Sr and Ba are shown as  
438 supporting information (11 figures and 1 Table). This material is available free of charge via  
439 the Internet at <http://pubs.acs.org>.

440

441 AUTHOR INFORMATION

442 **Corresponding Author**

443 \*K. Benzerara. Email: [karim.benzerara@impmc.upmc.fr](mailto:karim.benzerara@impmc.upmc.fr). Tel: +33 1-44-27-75-42

444 **Notes**

445 The authors declare no competing financial interest.

446 **Author Contributions**

447 The manuscript was written through contributions of all authors. All authors have given  
448 approval to the final version of the manuscript.

449 ACKNOWLEDGMENTS

450 Nithavong Cam was supported by French state funds managed by the ANR within the  
451 Investissements d'Avenir program under reference ANR-11-IDEX-0004-02 (Cluster of  
452 Excellence MATISSE). Karim Benzerara has been supported by funding from the European  
453 Research Council under the European Community's Seventh Framework Programme  
454 (FP7/2007-2013 Grant Agreement no.307110 - ERC CALCYAN). The TEM facility at



455 IMPMC was purchased owing to a support by Region Ile-de-France grant SESAME 2000 E  
456 1435.

457

## 458 REFERENCES

- 459 (1) McDonough, W. F.; Sun, S. The composition of the Earth. *Chem. Geol.* **1995**, *120* (3–4),  
460 223–253.
- 461 (2) Odum, H. T. Notes on the Strontium Content of Sea Water, Celestite Radiolaria, and  
462 Strontianite Snail Shells. *Science* **1951**, *114* (2956), 211–213.
- 463 (3) Walker, J. B. Inorganic micronutrient requirements of *Chlorella*: I. Requirements for  
464 calcium (or strontium), copper, and molybdenum. *Arch. Biochem. Biophys.* **1953**, *46* (1),  
465 1–11.
- 466 (4) Bowen, H. J. M.; Dymond, J. A. Strontium and Barium in Plants and Soils. *Proc. R. Soc.*  
467 *Lond. B Biol. Sci.* **1955**, *144* (916), 355–368.
- 468 (5) Dahl, S. G.; Allain, P.; Marie, P. J.; Murras, Y.; Boivin, G.; Ammann, P.; Tsouderos, Y.;  
469 Delmas, P. D.; Christiansen, C. Incorporation and distribution of strontium in bone.  
470 *Bone* **2001**, *28* (4), 446–453.
- 471 (6) Reginster, J. Y.; Deroisy, R.; Dougados, M.; Jupsin, I.; Colette, J.; Roux, C. Prevention  
472 of Early Postmenopausal Bone Loss by Strontium Ranelate: The Randomized, Two-  
473 Year, Double-Masked, Dose-Ranging, Placebo-Controlled PREVOS Trial. *Osteoporos.*  
474 *Int.* **2002**, *13* (12), 925–931.
- 475 (7) Verberckmoes, S. C.; Broe, M. E. D.; D’Haese, P. C. Dose-dependent effects of  
476 strontium on osteoblast function and mineralization. *Kidney Int.* **2003**, *64* (2), 534–543.
- 477 (8) Vakulovsky, S. M.; Nikitin, A. I.; Chumichev, V. B.; Katrich, I. Y.; Voitsekhovich, O.  
478 A.; Medinets, V. I.; Pisarev, V. V.; Bovkum, L. A.; Khersonsky, E. S. Cesium-137 and  
479 strontium-90 contamination of water bodies in the areas affected by releases from the  
480 chernobyl nuclear power plant accident: an overview. *J. Environ. Radioact.* **1994**, *23* (2),  
481 103–122.
- 482 (9) Casacuberta, N.; Masqué, P.; Garcia-Orellana, J.; Garcia-Tenorio, R.; Buesseler, K. O.  
483 <sup>90</sup>Sr and <sup>89</sup>Sr in seawater off Japan as a consequence of the Fukushima Dai-ichi nuclear  
484 accident. *Biogeosciences* **2013**, *10* (6), 3649–3659.
- 485 (10) Manos, M. J.; Ding, N.; Kanatzidis, M. G. Layered metal sulfides: Exceptionally  
486 selective agents for radioactive strontium removal. *Proc. Natl. Acad. Sci.* **2008**, *105* (10),  
487 3696–3699.
- 488 (11) Fukuda, S.; Iwamoto, K.; Atsumi, M.; Yokoyama, A.; Nakayama, T.; Ishida, K.; Inouye,  
489 I.; Shiraiwa, Y. Global searches for microalgae and aquatic plants that can eliminate  
490 radioactive cesium, iodine and strontium from the radio-polluted aquatic environment: a  
491 bioremediation strategy. *J. Plant Res.* **2014**, *127* (1), 79–89.
- 492 (12) Singh, S.; Eapen, S.; Thorat, V.; Kaushik, C. P.; Raj, K.; D’Souza, S. F.  
493 Phytoremediation of <sup>137</sup>Cs and <sup>90</sup>Sr from solutions and low-level nuclear waste by  
494 *Vetiveria zizanioides*. *Ecotoxicol. Environ. Saf.* **2008**, *69* (2), 306–311.
- 495 (13) Phillips, E.J.; Landa, E.R.; Kraemer, T.. Sulfate-Reducing Bacteria Release Barium and  
496 Radium from Naturally Occurring Radioactive Material in Oil-Field Barite.  
497 *Geomicrobiol. J.* **2001**, *18* (2), 167–182.

- 498 (14) Magalhães, M. O. L.; Sobrinho, N. M. B. do A.; Zonta, E.; Lima, L. da S.; Paiva, F. S.  
499 D. de. Mobilidade de bário em solo tratado com sulfato de bário sob condição de  
500 oxidação e redução. *Quím. Nova* **2011**, *34* (9), 1544–1549.
- 501 (15) Reeves, A. L. Barium. *Handb. Toxicol. Met.* **1986**, *2*, 84–94.
- 502 (16) Baldi, F.; Pepi, M.; Burrini, D.; Kniewald, G.; Scali, D.; Lanciotti, E. Dissolution of  
503 Barium from Barite in Sewage Sludges and Cultures of *Desulfovibrio desulfuricans*.  
504 *Appl. Environ. Microbiol.* **1996**, *62* (7), 2398–2404.
- 505 (17) Peek, S.; Clementz, M.T. Sr/Ca and Ba/Ca variations in environmental and biological  
506 sources: A survey of marine and terrestrial systems. *Geochim. Cosmochim. Acta* **2012**,  
507 *95*, 36-52.
- 508 (18) Sih, T.L.; Kingsford, M.J. Near-reef elemental signals in the otoliths of settling  
509 *Pomacentrus amboinensis* (Pomacentridae). *Coral Reefs*. **2016**, *35* (1), 303-315.
- 510 (19) Bahr, A.; Schonfeld, J.; Hoffmann, J.; Voigt, S.; Aurahs, R.; Kucera, M.; Flogel, S.;  
511 Jentzen, A.; Gerdes, A. Comparison of Ba/Ca and delta O-18(water) as freshwater  
512 proxies: A multi-species core-top study on planktonic foraminifera from the vicinity of  
513 the Orinoco River mouth. *Earth and Planet. Sci Lett.* **2013**, *383*, 45-57.
- 514 (20) Paytan, A.; Griffith, E.M. Marine barite: recorder of variations in ocean export  
515 productivity. *Deep-Sea Res. II*, **2007**, *54*, 687–705.
- 516 (21) von Allmen, K.; Böttcher, M.E.; Samankassou E., Nägler T.F. Barium isotope  
517 fractionation in the global barium cycle: First evidence from barium minerals and  
518 precipitation experiments. *Chem. Geol.* **2010**, *277*, 70-77.
- 519 (22) Cao, Z.; Siebert, C.; Hathorne, E.C.; ; Dai, M.H.; Frank, M. Constraining the oceanic  
520 barium cycle with stable barium isotopes. *Earth and Planet. Sci Lett.* **2016**, *434*, 1-9.
- 521 (23) Griffith, E.M.; Paytan, A. Barite in the ocean – occurrence, geochemistry and  
522 palaeoceanographic applications. *Sedim.*, 2012, *59*, 1817-1835.
- 523 (24) Frančišković-Bilinski, S.; Bilinski, H.; Grbac, R.; Žunić, J.; Nečemer, M.; Hanžel, D.  
524 Multidisciplinary work on barium contamination of the karstic upper Kupa River  
525 drainage basin (Croatia and Slovenia); calling for watershed management. *Environ.*  
526 *Geochem. Health* **2007**, *29* (1), 69–79.
- 527 (25) Pohl, P.; Schimmack, W. Adsorption of Radionuclides (<sup>134</sup>Cs, <sup>85</sup>Sr, <sup>226</sup>Ra, <sup>241</sup>Am) by  
528 Extracted Biomasses of Cyanobacteria (*Nostoc carneum*, *N. insulare*, *Oscillatoria*  
529 *geminata* and *Spirulina laxis-Sima*) and Phaeophyceae (*Laminaria digitata* and *L.*  
530 *japonica*; Waste Products from Alginate Production) at Different pH. *J. Appl. Phycol.*  
531 **2006**, *18* (2), 135–143.
- 532 (26) Dabbagh, R.; Ghafourian, H.; Baghvand, A.; Nabi, G. R.; Riahi, H.; Ahmadi Faghieh, M.  
533 A. Bioaccumulation and biosorption of stable strontium and <sup>90</sup>Sr by *Oscillatoria*  
534 *homogenea* cyanobacterium. *J. Radioanal. Nucl. Chem.* **2007**, *272* (1), 53–59.
- 535 (27) Liu, M.; Dong, F.; Kang, W.; Sun, S.; Wei, H.; Zhang, W.; Nie, X.; Guo, Y.; Huang, T.;  
536 Liu, Y. Biosorption of Strontium from Simulated Nuclear Wastewater by *Scenedesmus*  
537 *spinosus* under Culture Conditions: Adsorption and Bioaccumulation Processes and  
538 Models. *Int. J. Environ. Res. Public Health* **2014**, *11* (6), 6099–6118.
- 539 (28) Lee, S. Y.; Jung, K.-H.; Lee, J. E.; Lee, K. A.; Lee, S.-H.; Lee, J. Y.; Lee, J. K.; Jeong, J.  
540 T.; Lee, S.-Y. Photosynthetic biomineralization of radioactive Sr via microalgal CO<sub>2</sub>  
541 absorption. *Bioresour. Technol.* **2014**, *172*, 449–452.
- 542 (29) Fujita, Y.; Redden, G. D.; Ingram, J. C.; Cortez, M. M.; Ferris, F. G.; Smith, R. W.  
543 Strontium incorporation into calcite generated by bacterial ureolysis I. *Geochim.*  
544 *Cosmochim. Acta* **2004**, *68* (15), 3261–3270.

- 545 (30) Achal, V.; Pan, X.; Zhang, D. Bioremediation of strontium (Sr) contaminated aquifer  
546 quartz sand based on carbonate precipitation induced by Sr resistant *Halomonas sp.*  
547 *Chemosphere* **2012**, *89* (6), 764–768.
- 548 (31) Lauchnor, E. G.; Schultz, L. N.; Bugni, S.; Mitchell, A. C.; Cunningham, A. B.; Gerlach,  
549 R. Bacterially Induced Calcium Carbonate Precipitation and Strontium Coprecipitation  
550 in a Porous Media Flow System. *Environ. Sci. Technol.* **2013**, *47* (3), 1557–1564.
- 551 (32) Nehrke, G.; Reichart, G. J.; Van Cappellen, P.; Meile, C.; Bijma, J. Dependence of  
552 calcite growth rate and Sr partitioning on solution stoichiometry: Non-Kossel crystal  
553 growth. *Geochim. Cosmochim. Acta* **2007**, *71* (9), 2240–2249.
- 554 (33) Langer, G.; Nehrke, G.; Thoms, S.; Stoll, H. Barium partitioning in coccoliths of  
555 *Emiliania huxleyi*. *Geochim. Cosmochim. Acta* **2009**, *73* (10), 2899–2906.
- 556 (34) Takahashi, S.; Aizawa, K.; Nakamura, S.; Nakayama, K.; Fujisaki, S.; Watanabe, S.;  
557 Satoh, H. Accumulation of alkaline earth metals by the green macroalga *Bryopsis*  
558 *maxima*. *BioMetals* **2015**, *28* (2), 391–400.
- 559 (35) Krejci, M. R.; Wasserman, B.; Finney, L.; McNulty, I.; Legnini, D.; Vogt, S.; Joester, D.  
560 Selectivity in biomineralization of barium and strontium. *J. Struct. Biol.* **2011**, *176* (2),  
561 192–202.
- 562 (36) Sternberg, E.; Tang, D.; Ho, T.-Y.; Jeandel, C.; Morel, F. M. M. Barium uptake and  
563 adsorption in diatoms. *Geochim. Cosmochim. Acta* **2005**, *69* (11), 2745–2752.
- 564 (37) Kaduková, J.; Virčíková, E. Comparison of differences between copper bioaccumulation  
565 and biosorption. *Environ. Int.* **2005**, *31* (2), 227–232.
- 566 (38) Avery, S. V.; Smith, S. L.; Ghazi, A. M.; Hoptroff, M. J. Stimulation of strontium  
567 accumulation in linoleate-enriched *Saccharomyces cerevisiae* is a result of reduced Sr<sup>2+</sup>  
568 efflux. *Appl. Environ. Microbiol.* **1999**, *65* (3), 1191–1197.
- 569 (39) Wilcock, J. R.; Perry, C. C.; Williams, R. J. P.; Mantoura, R. F. C. Crystallographic  
570 and Morphological Studies of the Celestite Skeleton of the Acantharian Species  
571 *Phyllostaurus siculus*. *Proc. R. Soc. Lond. B Biol. Sci.* **1988**, *233* (1273), 393–405.
- 572 (40) Schröter, K.; Läuchli, A.; Sievers, A. Mikroanalytische Identifikation von Bariumsulfat-  
573 Kristallen in den Statolithen der Rhizoide von *Chara fragilis*, Desv. *Planta* **1975**, *122*  
574 (3), 213–225.
- 575 (41) Hemmersbach, R.; Volkmann, D.; Häder, D.-P. Graviorientation in Protists and Plants.  
576 *J. Plant Physiol.* **1999**, *154* (1), 1–15.
- 577 (42) Gooday, A. J.; Nott, J. A. Intracellular Barite Crystals in Two Xenophyophores,  
578 *Aschemonella ramuliformis* and *Galatheaemmina sp.* (Protozoa: Rhizopoda) With  
579 Comments on the Taxonomy of *A. Ramuliformis*. *J. Mar. Biol. Assoc. U. K.* **1982**, *62*  
580 (3), 595–605.
- 581 (43) Couradeau, E.; Benzerara, K.; Gerard, E.; Moreira, D.; Bernard, S.; Brown, G. E.;  
582 Lopez-Garcia, P. An Early-Branching Microbialite Cyanobacterium Forms Intracellular  
583 Carbonates. *Science* **2012**, *336* (6080), 459–462.
- 584 (44) Li, J.; Margaret Oliver, I.; Cam, N.; Boudier, T.; Blondeau, M.; Leroy, E.; Cosmidis, J.;  
585 Skouri-Panet, F.; Guigner, J.-M.; Féraud, C.; et al. Biomineralization Patterns of  
586 Intracellular Carbonatogenesis in Cyanobacteria: Molecular Hypotheses. *Minerals* **2016**,  
587 *6* (1), 10.
- 588 (45) Cam, N.; Georgelin, T.; Jaber, M.; Lambert, J.-F.; Benzerara, K. In vitro synthesis of  
589 amorphous Mg-, Ca-, Sr- and Ba-carbonates: What do we learn about intracellular  
590 calcification by cyanobacteria? *Geochim. Cosmochim. Acta* **2015**, *161*, 36–49.
- 591 (46) Benzerara, K.; Skouri-Panet, F.; Li, J.; Féraud, C.; Gugger, M.; Laurent, T.; Couradeau,  
592 E.; Ragon, M.; Cosmidis, J.; Menguy, N.; et al. Intracellular Ca-carbonate  
593 biomineralization is widespread in cyanobacteria. *Proc. Natl. Acad. Sci.* **2014**, *111* (30),  
594 10933–10938.

- 595 (47) Ragon, M.; Benzerara, K.; Moreira, D.; Tavera, R.; Lopez-Garcia, P. 16S rDNA-based  
596 analysis reveals cosmopolitan occurrence but limited diversity of two cyanobacterial  
597 lineages with contrasted patterns of intracellular carbonate mineralization. *Front.*  
598 *Microbiol.* **2014**, *5*, 331.
- 599 (48) Rippka, R.; Deruelles, J.; Waterbury, J. B.; Herdman, M.; Stanier, R. Y. Generic  
600 Assignments, Strain Histories and Properties of Pure Cultures of Cyanobacteria. *J. Gen.*  
601 *Microbiol.* **1979**, *111* (1), 1–61.
- 602 (49) Jaquet, J.-M.; Nirel, P.; Martignier, A. Preliminary investigations on picoplankton-  
603 related precipitation of alkaline-earth metal carbonates in meso-oligotrophic Lake  
604 Geneva (Switzerland). *J. Limnol.* **2013**, *72* (3), 592–605.
- 605 (50) Fernandez-Martinez, A.; Kalkan, B.; Clark, S. M.; Waychunas, G. A. Pressure-Induced  
606 Polyamorphism and Formation of “Aragonitic” Amorphous Calcium Carbonate. *Angew.*  
607 *Chem. Int. Ed.* **2013**, *52* (32), 8354–8357.
- 608 (51) Krejci, M. R.; Finney, L.; Vogt, S.; Joester, D. Selective Sequestration of Strontium in  
609 Desmid Green Algae by Biogenic Co-precipitation with Barite. *ChemSusChem* **2011**, *4*  
610 (4), 470–473.
- 611 (52) Kirichok, Y.; Krapivinsky, G.; Clapham, D. E. The mitochondrial calcium uniporter is a  
612 highly selective ion channel. *Nature* **2004**, *427* (6972), 360–364.
- 613 (53) Reusch, R. N.; Huang, R.; Bramble, L. L. Poly-3-hydroxybutyrate/polyphosphate  
614 complexes form voltage-activated Ca<sup>2+</sup> channels in the plasma membranes of  
615 *Escherichia coli*. *Biophys. J.* **1995**, *69* (3), 754–766.
- 616 (54) Vrettos, J. S.; Stone, D. A.; Brudvig, G. W. Quantifying the Ion Selectivity of the Ca<sup>2+</sup>  
617 Site in Photosystem II: Evidence for Direct Involvement of Ca<sup>2+</sup> in O<sub>2</sub> Formation †.  
618 *Biochemistry (Mosc.)* **2001**, *40* (26), 7937–7945.
- 619 (55) Falke, J. J.; Snyder, E. E.; Thatcher, K. C.; Voertler, C. S. Quantitating and engineering  
620 the ion specificity of an EF-hand-like calcium binding site. *Biochemistry (Mosc.)* **1991**,  
621 *30* (35), 8690–8697.
- 622 (56) Henikoff, S.; Greene, E. A.; Pietrokovski, S.; Bork, P.; Attwood, T. K.; Hood, L. Gene  
623 Families: The Taxonomy of Protein Paralogs and Chimeras. *Science* **1997**, *278* (5338),  
624 609–614.
- 625 (57) Gonzalez-Muñoz, M. T.; Martinez-Ruiz, F.; Morcillo, F.; Martin-Ramos, J. D.; Paytan,  
626 A. Precipitation of barite by marine bacteria: A possible mechanism for marine barite  
627 formation. *Geology* **2012**, *40* (8), 675–678.
- 628 (58) Kreger, D. R.; Boéré, H. Some Observations on Barium Sulphate in Spirogyra\*. *Acta*  
629 *Bot. Neerlandica* **1969**, *18* (1), 143–151.

630

631

632